JOURNAL OF SOLID STATE CHEMISTRY **110**, 43–49 (1994)

# A Trivalent Vanadium Monophosphate with a Tunnel Structure: $Cd_3V_4(PO_4)_6$

S. Boudin, A. Grandin, M. M. Borel, A. Leclaire, and B. Raveau

*Laboratoire CRISMAT, ISMRa, Université de Caen, Boulevard du Maréchal Juin, 14050 Caen Cedex, France*

Received April 19, 1993; in revised form July 23, 1993; accepted July 27, 1993

**A new vanadium(III) monophosphate, $Cd_3V_4(PO_4)_6$, has been isolated and its structure has been determined from single-crystal X-ray diffraction data. It crystallizes in the monoclinic space group *C2/c* with $a = 12.446(1)$ Å, $b = 12.547(1)$ Å, $c = 6.487(1)$ Å, and $\beta = 115.66°(1)$. The three-dimensional framework $[V_4P_6O_{24}]_\infty$ is built from bi-octahedral $V_2O_{10}$ units linked through monophosphate groups. It can be described as the stacking of $[V_2P_2O_{12}]_\infty$ layers, parallel to (100) connected through layers of $PO_4$ tetrahedra. The $[V_2P_2O_{12}]_\infty$ layers are themselves formed of $[VPO_8]_\infty$ chains running along c, connected through the corners of their polyhedra and the edges of the $VO_6$ octahedra alternately. This structure forms small tunnels running along [001], [110], and [1$\bar{1}$0], where the cadmium ions are located with distorted octahedral and trigonal prismatic coordinations. In fact, the $[Cd_3V_4P_6O_{24}]_\infty$ framework forms large empty tunnels running along [001].** © 1994 Academic Press, Inc.

## INTRODUCTION

Phosphates of trivalent vanadium form a family of about 13 compounds which exhibit various structures. Most of them are characterized by isolated $VO_6$ octahedra, i.e., by octahedra linked to $PO_4$ groups only. This is indeed the case for the diphosphates $AVP_2O_7$ with $A$ = Cs (1), Rb (2), K (3), Na (4), and Li (5), and $AV_2(P_2O_7)_2$ with $A$ = Sr (6) and Ba (7), for the mixed phosphate $Ca_2V(PO_4)P_2O_7$ (8), for the monophosphate $K_6V_2(PO_4)_4$ (9), and for the polyphosphates $V(PO_3)_3$ (10) and $CsV_2O(PO_3)_5$ (11). In addition to this large series there exist some V(III) phosphates involving bi-octahedral units of edge- or face-sharing $VO_6$ octahedra but they are rather rare. In fact, the mixed phosphate $KV_4(PO_4)(P_2O_7)(P_4O_{13})$ (12) is the only example of V(III) phosphate built from isolated structural units $V_2O_{10}$ of two edge-sharing octahedra.

During our recent investigation of the system Cd–V–P–O, a new phase was observed in addition to the vanadium (IV) monophosphates $Cd(VO)_2(PO_4)_2$ (13, 14) and the mixed valent phosphate $Cd_5V_2(VO)(PO_4)_6$ (15). We report here the synthesis and crystal structure of this compound, which is a trivalent monophosphate with the formula $Cd_3V_4(PO_4)_6$.

## EXPERIMENTAL

Yellow single crystals of $Cd_3V_4(PO_4)_6$ were isolated from a mixture of nominal composition: "$CdV_2P_2O_8$." The crystal growth was performed in two steps. First, a mixture of CdO, $H(NH_4)_2PO_4$, and $V_2O_5$ at a molar ratio of 5 : 2 : 10 was heated to 650 K in order to eliminate $NH_3$ and $H_2O$.

Second, the resulting finely ground product was mixed with an appropriate amount of vanadium and sealed in an evacuated silica ampoule. This sample was heated to 1223 K for 24 hr, slowly cooled at a rate of 1 K $hr^{-1}$ to 1073 K, and then quenched at room temperature.

The composition of this phase, deduced from the structural determination to be $Cd_3V_4P_6O_{24}$, was confirmed by microprobe analysis. Subsequent attempts to prepare a pure phase were unsuccessful; one always obtained a mixture of this new phase with the orthorhombic form of the monophosphate $Cd(VO)_2(PO_4)_2$ (14).

## STRUCTURE DETERMINATION

A yellow crystal of $Cd_3V_4(PO_4)_6$ with dimensions 0.103 × 0.032 × 0.019 mm was selected for the structure determination. The cell parameters reported in Table 1 were determined and refined by diffractometric techniques at 294 K with a least-squares refinement based upon 25 reflections with $18 < \theta \leq 22°$. The systematic absences $h + k = 2n + 1$ for all the $h\ k\ l$ and $l = 2n + 1$ for $h\ 0\ l$ are consistent with the space groups *C2/c* and *Cc*.

The Harker peaks present in the Patterson function are characteristic of the centrosymmetric space group *C2/c*. The data were collected on a CAD-4 Enraf–Nonius automatic diffractometer with the measurement parameters reported in Table 1.

The reflections were corrected for Lorentz and polar-

0022-4596/94 $6.00

TABLE 1
Summary of Crystal Data Intensity, Measurements, and Structure Refinement Parameters for $Cd_3V_4(PO_4)_6$

| | |
|---|---|
| Crystal data | |
| Space group | $C2/c$ |
| Cell dimensions | $a$ = 12.446(1) Å<br>$b$ = 12.547(2) Å, $\beta$ = 115.66(1)°<br>$c$ = 6.487(1) Å |
| Volume | 913(1) $Å^3$ |
| $Z$ | 2 |
| Intensity measurements | |
| $\lambda(MoK\alpha)$ | 0.71073 Å |
| Scan mode | $\omega - \theta$ |
| Scan width (°) | $1 + \tan\theta$ |
| Slit aperture (mm) | $1 + \tan\theta$ |
| Max $\theta$(°) | 45 |
| Standard reflections | 3 measured every 3000 sec |
| Reflections with $I > 3\sigma$ | 1157 |
| $\mu(mm^{-1})$ | 5.38 |
| Structure solution and refinement | |
| Parameters refined | 93 |
| Agreement factors | $R = 0.047$, $R_w = 0.046$ |
| Weighting scheme | $w = f(\sin\theta/\lambda)$ |
| $\Delta/\sigma$ max | 0.004 |
| $\Delta\rho(eÅ^{-3})$ | 2.5 |

ization and secondary extinction effects. No absorption corrections were performed.

The structure was solved with the heavy atom method. The refinement of the atomic coordinates and the anisotropic thermal factors led to $R = 0.047$ and $R_w = 0.046$ and to the atomic parameters shown in Table 2.

TABLE 2
Positional Parameters and Their Estimated Standard Deviations

| Atom | $x$ | $y$ | $z$ | $B(Å^2)$ |
|---|---|---|---|---|
| Cd(1) | 0.5 | 0.25198(7) | 0.25 | 1.006(8) |
| Cd(2)[a] | 0.0208(1) | −0.0003(1) | 0.4637(3) | 0.67(2) |
| V | 0.27756(7) | 0.15402(8) | 0.3676(1) | 0.38(1) |
| P(1) | 0.2478(1) | 0.3927(1) | 0.1395(3) | 0.80(2) |
| P(2) | 0 | 0.2189(2) | 0.25 | 0.78(3) |
| O(1) | 0.3200(4) | 0.1615(4) | 0.0950(9) | 1.26(8) |
| O(2) | 0.2318(4) | 0.3213(5) | 0.3204(9) | 1.26(8) |
| O(3) | 0.2988(5) | 0.0052(5) | 0.358(1) | 1.65(9) |
| O(4) | 0.4457(4) | 0.2096(5) | 0.5346(9) | 1.23(8) |
| O(5) | 0.0945(5) | 0.1457(5) | 0.229(1) | 1.72(9) |
| O(6) | 0.3821(4) | 0.3979(5) | 0.202(1) | 1.46(9) |

*Note.* Anisotropically refined atoms are given in the isotropic equivalent displacement parameter defined as $B = 4/3\ [\beta_{11}a^2 + \beta_{22}b^2 + \beta_{33}c^2 + \beta_{12}ab\cos\gamma + \beta_{13}ac\cos\beta + \beta_{23}bc\cos\alpha]$.

[a] Occupation factor = 0.25.

## DESCRIPTION OF THE STRUCTURE AND DISCUSSION

The projection of the structure of this new phase along **b** (Fig. 1) and **c** (Fig. 2) shows that the three-dimensional framework $[V_4P_6O_{24}]_\infty$ consists of corner-sharing $VO_6$ octahedra and $PO_4$ tetrahedra. It can be seen that each $PO_4$ tetrahedron shares its corners with $VO_6$ octahedra only, whereas two $VO_6$ octahedra share one edge, forming "$V_2O_{10}$" units that are isolated, i.e., linked through $PO_4$ tetrahedra. Thus, this compound is a monophosphate of V(III) represented by the formula $Cd_3V_4(PO_4)_6$.

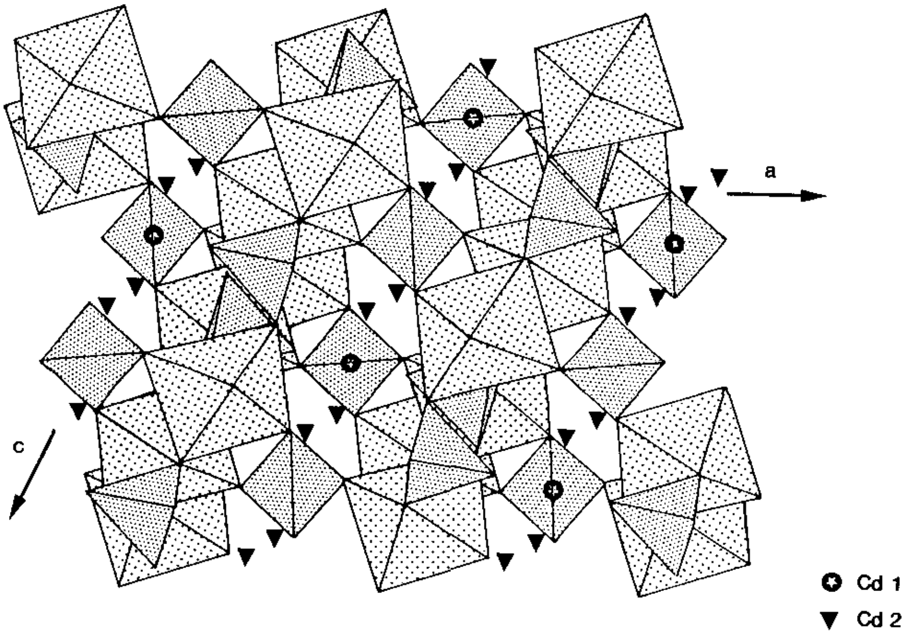

FIG. 1. Projection of the structure along **b**.

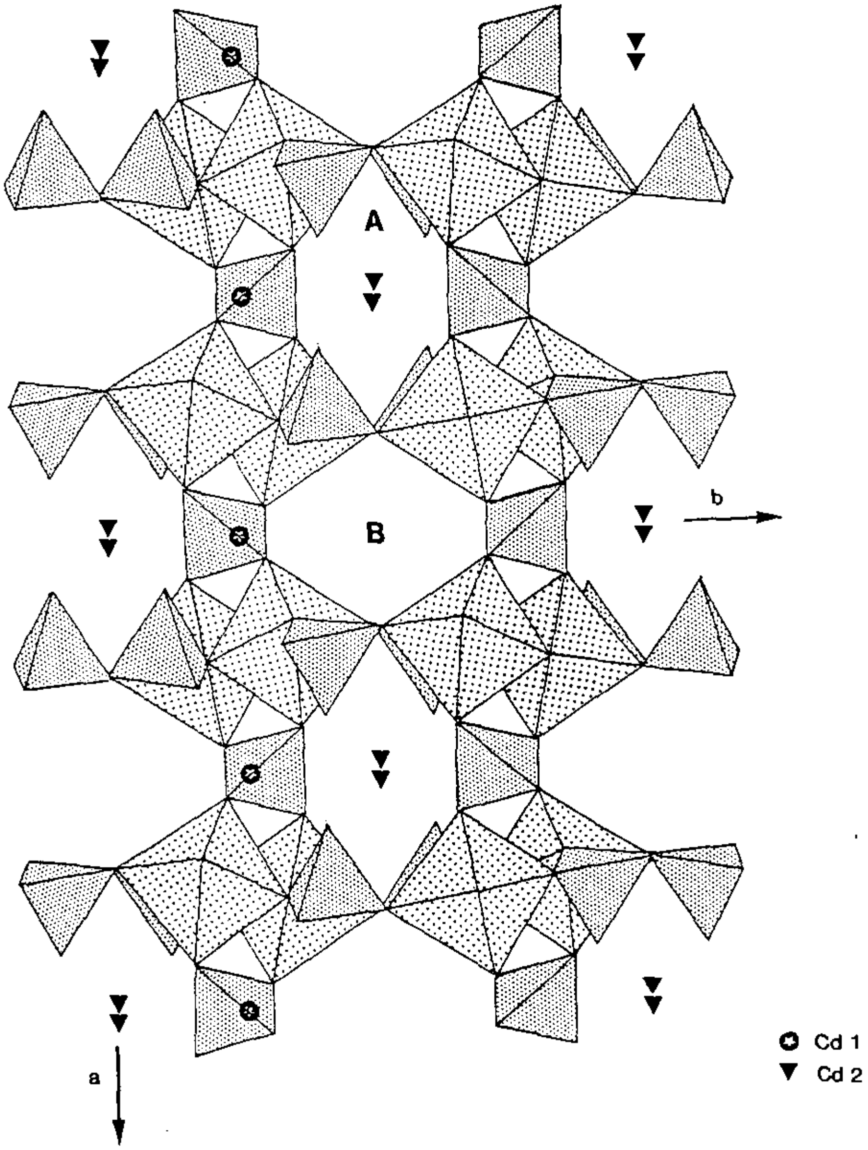

FIG. 2. Projection of the structure along c, showing the two types of tunnels.

The projection of half a cell of this structure perpendicular to the (100) plane (Fig. 3) shows the arrangement of the "$V_2O_{10}$" units in the (100) plane. Note the similarity with the structure of the V(IV) diphosphate $(VO)_2P_2O_7$ (16) (Fig. 4). In both structures one observes "$V_2O_{10}$" units linked through $PO_4$ tetrahedra in such a way that some oxygens are triply bonded, i.e., shared between one $PO_4$ tetrahedron and two $VO_6$ octahedra. However, in $(VO)_2$ $P_2O_7$ the "$V_2O_{10}$" units are all parallel (Fig. 4), whereas they form a fishbone array in $Cd_3V_4(PO_4)_6$ (Fig. 3). In the latter structure the $V_2O_{10}$ units and $PO_4$ tetrahedra form $[V_2P_2O_{14}]_\infty$ ribbons running along **c** that are one bi-octahedral unit wide. Such ribbons share the corners of their polyhedra in the (100) plane in such a way that the "$V_2O_{10}$" units of two successive ribbons are oriented at 90°. Thus the $[V_2P_2O_{14}]_\infty$ ribbons form $[V_2P_2O_{12}]_\infty$ layers parallel to (001), where the fourth apices of the $PO_4$ tetrahedra of the successive $[V_2P_2O_{14}]_\infty$ ribbons are alternately pointing below and above the mean plane of the $[V_2P_2O_{12}]_\infty$ layer (Fig. 3).

In fact, the $[V_2P_2O_{12}]_\infty$ layers can be described by the assemblage of $[VPO_8]_\infty$ chains running along **c**. Such chains (Fig. 5a), in which one $PO_4$ tetrahedron alternates with one $VO_6$ octahedron, are classically observed in many phosphates of transition elements (17–23). In the present structure they are associated either by the corners of their polyhedra or by the edges of their $VO_6$ octahedra, forming double $[V_2P_2O_{14}]_\infty$ chains (Fig. 5b) also observed

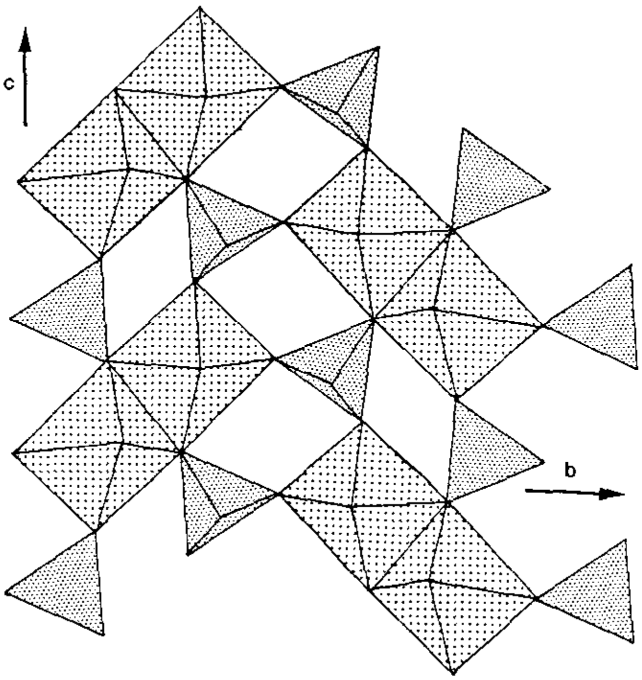

FIG. 3. Projection of half a cell of this structure perpendicular to the (100) plane.

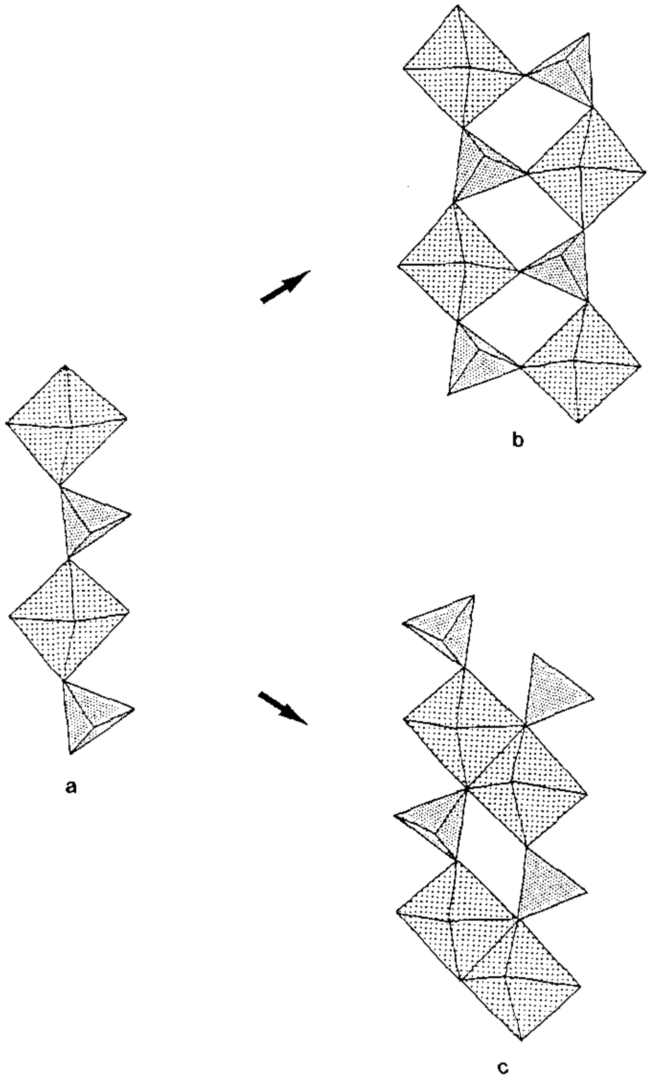

FIG. 5. (a) The $[VPO_8]_\infty$ chain, (b) the $[V_2P_2O_{14}]_\infty$ double chain, and (c) the $[V_2P_2O_{14}]_\infty$ ribbon.

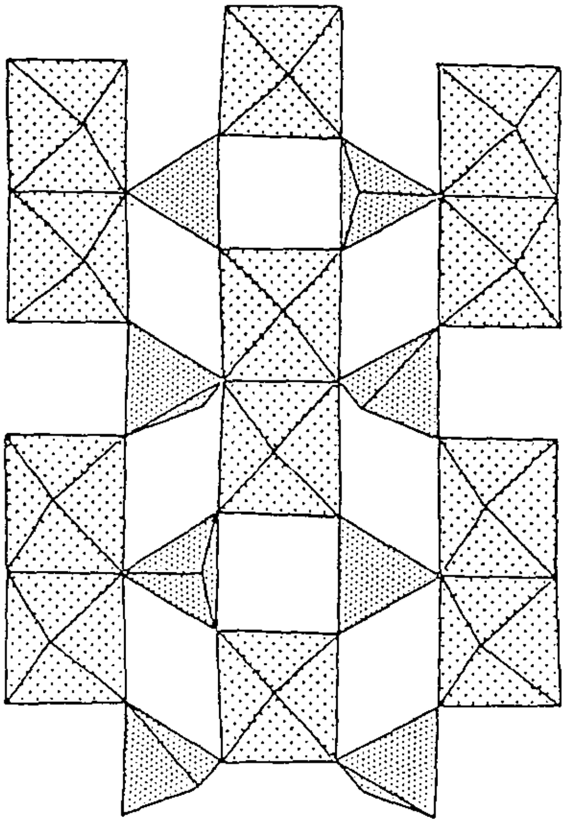

FIG. 4. Projection of the $(VO)_2P_2O_7$ structure along **a**.

in many monophosphates of transition elements or the $[V_2P_2O_{14}]_\infty$ ribbons (Fig. 5c), respectively. Thus the $[V_2P_2O_{12}]_\infty$ layers (Fig. 3) can be described either from $[V_2P_2O_{14}]_\infty$ double chains sharing the edges of their octahedra or from $[V_2P_2O_{14}]_\infty$ ribbons sharing the corners of their polyhedra. It is also worth noting that the $PO_4$ tetrahedra P(1) of the $[V_2P_2O_{12}]_\infty$ layers have their fourth apex free as shown from the projection of the structure along **c** (Fig. 2).

The latter view of the structure along **c** (Fig. 2) shows also that the $[V_4P_6O_{24}]_\infty$ framework consists of a regular stacking of identical $[V_2P_2O_{12}]_\infty$ layers connected through layers of $PO_4$ tetrahedra (labeled P(2)). In fact, in two successive (100) $[V_2P_2O_{12}]_\infty$ layers the "$V_2O_{10}$" units are oriented in a different way, i.e., are turned 90° with respect to each other. This orientation can easily be understood

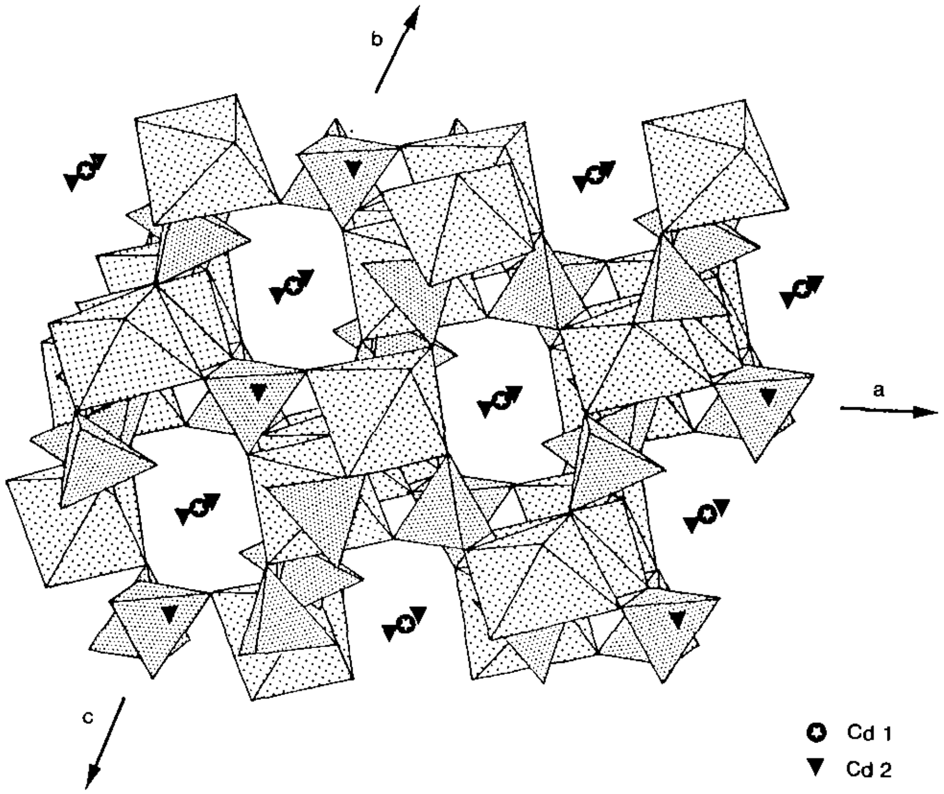

FIG. 6. *Projection of the structure along the [011] direction.*

by viewing the structure along the [011] direction (Fig. 6). The latter projection shows that the P(2) tetrahedra, which ensure the junction between two $[V_2P_2O_{12}]_\infty$ layers, share two opposite edges with $V_2O_{10}$ units of two successive layers; as a result one observes $[V_2PO_{10}]_\infty$ columns (Fig. 7) running along the direction perpendicular to the (100) plane in which the $V_2O_{10}$ units are alternately turned 90° with respect to each other.

The $[V_4P_6O_{24}]_\infty$ framework induces series of tunnels along **c** (labeled A and B *in* Fig. 2) and [011], [0$\bar{1}$1] directions (Fig. 6). The [001]-A tunnels and [011], [0$\bar{1}$1] tunnels, which are bordered by the free oxygen atoms of the P(1) tetrahedra, are fully occupied by the cadmium ions. The Cd(1) ions, which are located at the intersection of the [011] and [0$\bar{1}$1] tunnels, exhibit a distorted octahedral coordination with Cd–O distances ranging from 2.286 to 2.317 Å (Fig. 8a). The Cd(2) ions which are located at the intersection of the [001]-A and [011] tunnels exhibit a prismatic trigonal coordination (Fig. 8b) with Cd–O distances ranging from 2.225 to 2.781 Å; only one intersection of two is randomly occupied. In fact, the short Cd–O distances show that this structure would not be described as a true tunnel structure if the [001] tunnels, labeled B, were not involved. The latter are indeed much larger and paradoxically empty (Fig. 2). Thus the $CdO_6$ octahedra

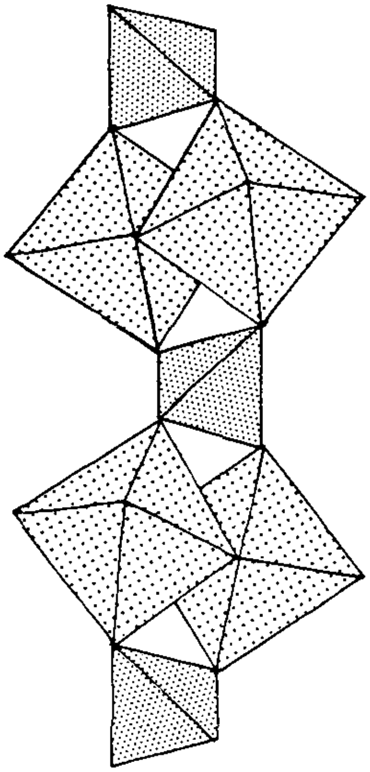

FIG. 7. The $[V_2PO_{10}]_\infty$ columns perpendicular to the (100) plane.

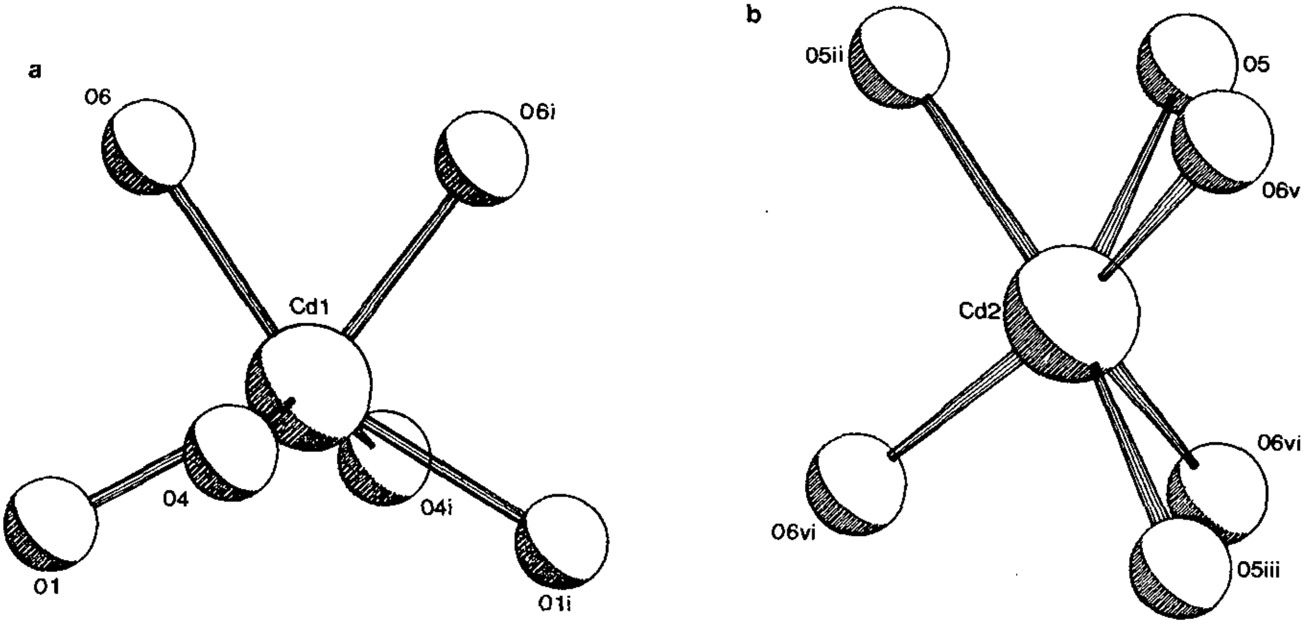

FIG. 8. (a) The Cd$^{2+}$ (1) environment and (b) the Cd$^{2+}$ (2) environment.

TABLE 3

Bond Distances (Å) and Angles (°) in the $Cd_3V_4(PO_4)_3$ Structure

| V | O(1) | O(2) | O(2$^{v}$) | O(3) | O(4) | O(5) |
|---|---|---|---|---|---|---|
| O(1) | 2.055(6) | 2.959(9) | 4.12(1) | 2.687(8) | 2.661(8) | 2.282(9) |
| O(2) | 89.1(2) | 2.162(6) | 2.82(1) | 4.04(1) | 2.789(8) | 2.692(9) |
| O(2$^{v}$) | 164.7(2) | 82.7(2) | 2.100(6) | 3.15(1) | 2.778(8) | 2.815(9) |
| O(3) | 85.8(3) | 170.6(3) | 104.1(3) | 1.890(7) | 3.07(1) | 2.903(8) |
| O(4) | 81.6(2) | 83.6(2) | 84.8(2) | 103.4(2) | 2.019(5) | 4.02(1) |
| O(5) | 105.9(3) | 79.3(2) | 85.2(3) | 94.6(3) | 161.1(2) | 2.058(6) |

| P(1) | O(1) | O(2) | O(3) | O(6) |
|---|---|---|---|---|
| O(1) | 1.542(6) | 2.494(8) | 2.540(8) | 2.530(8) |
| O(2) | 107.2(3) | 1.556(6) | 2.536(9) | 2.501(8) |
| O(3) | 111.6(3) | 110.6(4) | 1.528(6) | 2.505(7) |
| O(6) | 110.3(4) | 107.7(4) | 109.3(3) | 1.542(5) |

| P(2) | O(4$^{v}$) | O(4$^{vii}$) | O(5) | O(5$^{ii}$) |
|---|---|---|---|---|
| O(4$^{v}$) | 1.547(6) | 2.52(1) | 2.563(8) | 2.508(9) |
| O(4$^{vii}$) | 109.2(5) | 1.547(6) | 2.508(9) | 2.563(8) |
| O(5) | 111.9(3) | 108.4(4) | 1.546(6) | 2.48(1) |
| O(5$^{ii}$) | 108.4(4) | 111.9(3) | 107.0(6) | 1.546(6) |

Cd(1)–O(1) : 2.317(5) Å
Cd(1)–O(1$^{i}$) : 2.317(5)
Cd(1)–O(4) : 2.286(6)
Cd(1)–O(4$^{i}$) : 2.286(6)
Cd(1)–O(6) : 2.282(6)
Cd(1)–O(6$^{i}$) : 2.282(6)

Cd(2)–O(5) : 2.781(8)
Cd(2)–O(5$^{ii}$) : 2.328(6)
Cd(2)–O(5$^{iii}$) : 2.400(6)
Cd(2)–O(6$^{iv}$) : 2.225(6)
Cd(2)–O(6$^{v}$) : 2.354(7)
Cd(2)–O(6$^{vi}$) : 2.318(6)

Symmetry codes:
i : $1 - x$ ; $y$ ; $1/2 - z$
ii : $-x$ ; $y$ ; $1/2 - z$
iii : $x$ ; $-y$ ; $z + 1/2$
iv : $x - 1/2$ ; $y - 1/2$ ; $z$
v : $1/2 - x$ ; $1/2 - y$ ; $1 - z$
vi : $1/2 - x$ ; $y - 1/2$ ; $1/2 - z$

and trigonal prisms can be considered as a part of the host lattice which should be written $[Cd_3V_4P_6O_{24}]_\infty$.

The interatomic distances observed for the $PO_4$ tetrahedra (Table 3) show that the P(1) tetrahedra are almost regular in spite of the existence of one free apex. Contrary to other phosphates such as $K_6V_2P_4O_{16}$ (9), $Na_2VP_2O_8$ (24), or $Na_5V_2P_3O_{14} \cdot H_2O$ (25), the P(1)–O(6) bond corresponding to this free apex is not short (1.542 Å); this is easily explained by the fact that oxygen atom is not really free, since it is strongly bonded to Cd(2).

The "$O_6$" octahedron surrounding the vanadium atom is very distorted, with O–O distances ranging from 2.687 to 3.282 Å; nevertheless the V–O distances are distributed in a rather short range, from 1.89 to 2.16 Å, in agreement with the usual behavior of V(III) in phosphates.

## CONCLUDING REMARKS

This structural study shows the second example of V(III) phosphates characterized by bi-octahedral $V_2O_{10}$ units. There is no doubt that the cadmium species, owing to their small size, can be considered part of the framework rather than insertion cations. One interesting feature of this structure is the existence of rather large tunnels, running along [001], which are empty. This suggests the possibility of interpolation nonstoichiometry, which should be obtained by introducing univalent cations in the structure in such a way that the trivalent oxidation state of vanadium is maintained.

## REFERENCES

1. Y. P. Wang and K. H. Lii, *Acta Crystallogr., Sect. C* **45,** 1210 (1991).
2. U. Flörke, *Z. Kristallogr.* **191,** 137 (1990).
3. L. Benhamada, A. Grandin, M. M. Borel, A. Leclaire, and B. Raveau, *Acta Crystallogr., Sect. C* **47,** 424 (1991).
4. Y. P. Wang, K. H. Lii, and S. L. Wang, *Acta Crystallogr., Sect. C* **45,** 673 (1989).
5. K. H. Lii, Y. P. Wang, B. Chen, and S. L. Wang, *J. Solid State Chem.* **86,** 143 (1990).
6. S. J. Hwu and E. D. Willis, *J. Solid State Chem.* **93,** 69 (1991).
7. L. Benhamada, A. Grandin, M. M. Borel, A. Leclaire, and B. Raveau, *Acta Crystallogr., Sect. C* **47,** 2437 (1991).
8. K. H. Lii, N. S. Wen, C. C. Su, and B. R. Chueh, *Inorg. Chem.* **31,** 439 (1992).
9. L. Benhamada, A. Grandin, M. M. Borel, A. Leclaire, and B. Raveau, *J. Solid State Chem.* **91,** 264 (1991).
10. B. C. Tofield, G. R. Crane, G. A. Pasteur, and R. C. Sherwood, *J. Chem. Soc.*, 1806 (1975).
11. B. Klinkert and M. Jansen, *Z. Anorg. Allg. Chem.* **567,** 87 (1988).
12. L. Benhamada, A. Grandin, M. M. Borel, A. Leclaire, and B. Raveau, *J. Solid State Chem.* **104,** 193 (1993).
13. A. Leclaire, A. Grandin, J. Chardon, M. M. Borel, and B. Raveau, *Eur. J. Solid State Inorg. Chem.* **30,** 393 (1993).
14. A. Leclaire, J. Chardon, A. Grandin, M. M. Borel, and B. Raveau, *Eur. J. Solid State Inorg. Chem.* **30,** 461 (1993).
15. P. Crespoa, A. Grandin, M. M. Borel, A. Leclaire, and B. Raveau, *J. Solid State Chem.* **105,** 307 (1993).
16. J. W. Jonson, D. C. Johnston, A. J. Jacobson, and J. F. Brody, *J. Am. Chem. Soc.* **106,** 8123 (1984).
17. K. H. Lii, C. H. Li, C. Y. Cheng, and S. L. Wang, *J. Solid State Chem.* **95,** 352 (1991).
18. K. H. Lii, C. H. Li, T. M. Cheng, and S. L. Wang, *Z. Kristallogr.* **197,** 67 (1991).
19. L. Behamada, A. Grandin, M. M. Borel, A. Leclaire, and B. Raveau, *C. R. Acad. Sci., Ser. 2* **314,** 585 (1992).
20. L. Benhamada, A. Grandin, M. M. Borel, A. Leclaire, and B. Raveau, *Acta Crystallogr., Sect. C* **47,** 1138 (1991).
21. I. Tordjman, R. Masse and J. C. Guitel, *Z. Kristallogr.* **139,** 103 (1974).
22. G. Costentin, M. M. Borel, A. Grandin, A. Leclaire, and B. Raveau, *J. Solid State Chem.* **95,** 168 (1991).
23. A. Benabbas, M. M. Borel, A. Grandin, J. Chardon, A. Leclaire, and B. Raveau, *J. Solid State Chem.* **91,** 323 (1991).
24. L. Benhamada, A. Grandin, M. M. Borel, A. Leclaire, and B. Raveau, *J. Solid State Chem.* **101,** 154 (1992).
25. L. Benhamada, A. Grandin, M. M. Borel, A. Leclaire, and B. Raveau, *J. Solid State Chem.* **96,** 390 (1992).